Drug Design, Development and Therapy

Dovepress
Taylor & Francis Group

Open Access Full Text Article

ORIGINAL RESEARCH

# DHLCA Alleviates Diabetic Kidney Disease via TGR5/FXR Activation and Gut Microbiota Remodeling

Hua Zhou[1,*], Xiaodie Mu[2,*], Huiyue Hu[1,*], Shuya Zhao[1], Nan Hu[3], Min Yang[1,*], Jingting Jiang[4–6,*]

[1]Department of Nephrology, The Third Affiliated Hospital of Soochow University, Changzhou, 213003, People's Republic of China; [2]Department of Nephrology, The Second People's Hospital of Hefei, Hefei, 230011, People's Republic of China; [3]Department of Pharmacy, The Third Affiliated Hospital of Soochow University, Changzhou, 213003, People's Republic of China; [4]Department of Tumor Biological Treatment, The Third Affiliated Hospital of Soochow University, Changzhou, 213003, People's Republic of China; [5]Jiangsu Engineering Research Center for Tumor Immunotherapy, The Third Affiliated Hospital of Soochow University, Changzhou, 213003, People's Republic of China; [6]Institute of Cell Therapy, The Third Affiliated Hospital of Soochow University, Changzhou, 213003, People's Republic of China

*These authors contributed equally to this work

Correspondence: Jingting Jiang, Department of Tumor Biological Treatment, Jiangsu Engineering Research Center for Tumor Immunotherapy, Institute of Cell Therapy, The Third Affiliated Hospital of Soochow University, Changzhou, People's Republic of China, Email jiangjingting@suda.edu.cn; Min Yang, Department of Nephrology, The Third Affiliated Hospital of Soochow University, Changzhou, People's Republic of China, Email yangmin1516@suda.edu.cn



**Purpose:** Diabetic kidney disease (DKD) is a major contributor to chronic kidney disease worldwide. Bile acids (BAs) are increasingly recognized as key regulators of glucose metabolism and kidney function. This study aimed to investigate the role of BA metabolism in the progression of DKD.

**Methods:** Plasma BA profiles were measured in healthy controls (HC), patients with type 2 diabetes mellitus (T2DM), and patients with DKD using ultra-high-performance liquid chromatography–tandem mass spectrometry (UPLC-MS/MS). After identifying potential BA biomarkers in the clinical cohort, in vivo validation was conducted using dehydrolithocholic acid (DHLCA) intervention in DKD mouse model. Kidney injury markers, as well as the expression of Takeda G protein-coupled receptor 5 (TGR5) and farnesoid X receptor (FXR), were evaluated. In addition, gut microbiota (GM) composition was analyzed via metagenomic sequencing following DHLCA treatment.

**Results:** The plasma DHLCA levels were significantly lower in DKD with macroalbuminuria group compared to T2DM group and DKD with microalbuminuria group ($P < 0.01$). Partial Spearman correlation analysis adjusted for age and diabetes duration showed that DHLCA levels were negatively correlated with urine albumin ($\rho = -0.347$; 95% CI, –0.531 to –0.135; q = 0.008) and urine albumin-to-creatinine ratio (UACR) ($\rho = -0.332$; 95% CI, –0.499 to –0.155; q = 0.010). In vivo, DHLCA administration significantly reduced UACR and fasting blood glucose (FBG) levels ($P < 0.01$), and improved liver function (ALT, $P < 0.05$) in DKD mice. DHLCA treatment attenuated renal tubular injury, restored TGR5 and FXR expression in kidney tissue, and decreased levels of kidney injury molecule-1 (KIM-1) and neutrophil gelatinase-associated lipocalin (NGAL). Metagenomic analysis revealed an enrichment of *Lachnospiraceae bacterium* following DHLCA treatment.

**Conclusion:** DHLCA may represent a promising therapeutic candidate for DKD by targeting the TGR5/FXR signaling pathway and GM remodeling. Its metabolic and kidney benefits, along with an improved hepatic profile and absence of hepatotoxicity, support further translational investigation.

**Keywords:** bile acid, diabetic kidney disease, farnesoid X receptor, gut microbiota, Takeda G protein-coupled receptor 5

## Introduction

Diabetes mellitus (DM) is linked with numerous complications across various organ systems, with diabetic kidney disease (DKD) being the most critical, leading to end-stage renal disease (ESRD).[1] Given the limited effectiveness of current treatments for DKD, continuous research is underway to uncover the molecular mechanisms behind renal damage and to create innovative medications.

Received: 7 May 2025
Accepted: 12 July 2025
Published: 29 July 2025

**Graphical Abstract**

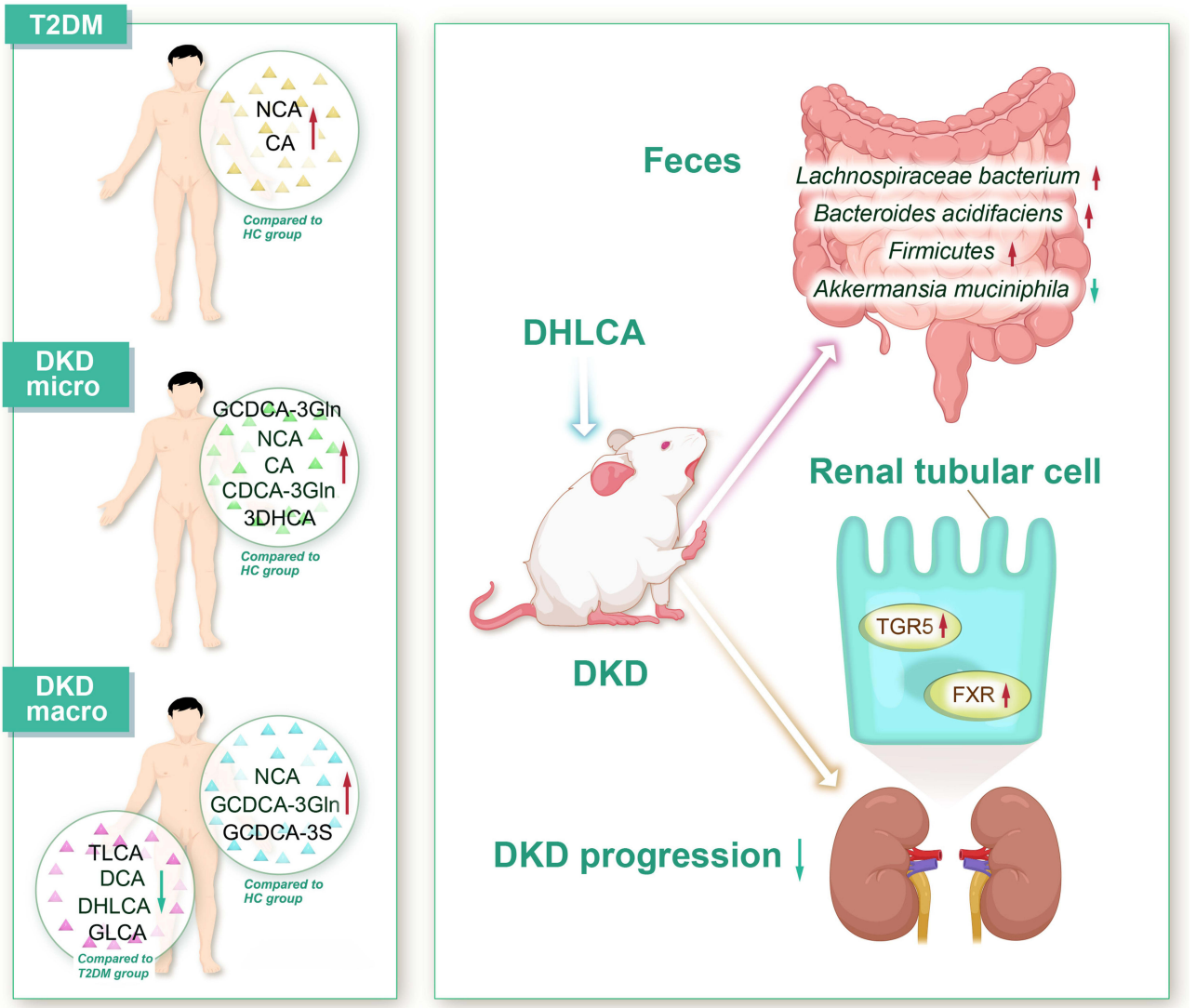


Recent metabolomic studies have revealed step-wise alterations in bile acid (BA) metabolism during the progression of DKD, suggesting that BA dysregulation may not only reflect disease severity but also contribute to its pathogenesis.[2] BAs exert biological effects through receptor-mediated signaling pathways, primarily via the farnesoid X receptor (FXR) and the Takeda G protein-coupled receptor 5 (TGR5).[3,4] Activation of FXR has been shown to prevent diabetic nephropathy by modulating lipid metabolism, reducing inflammation and fibrosis, and suppressing oxidative stress.[5] Similarly, TGR5 activation has been linked to mitochondrial biogenesis, enhancement of antioxidant responses, and inhibition of kidney injury in diabetes.[6] However, the expression patterns and kidney-specific functions of these receptors in DKD remain incompletely characterized.

Mounting evidence suggests that gut microbiota (GM)–BA interactions play a pivotal role in modulating host metabolism and kidney health.[3,7–9] Given this bidirectional relationship, disturbances in the GM-BA axis may represent a critical link between intestinal dysbiosis and DKD progression.[10] Despite these insights, several knowledge gaps remain unresolved, including: (i) the temporal dynamics and functional implications of individual BAs across DKD stages; (ii) the mechanistic role of GM-BA interactions in modulating BA receptor signaling within the kidney; and (iii) the therapeutic potential of secondary BAs as endogenous agonists of FXR/TGR5.

This study proposes the hypothesis that dehydrolithocholic acid (DHLCA), a secondary BA, ameliorates renal tubular injury and proteinuria in DKD through dual activation of FXR and TGR5 and concurrent remodeling of GM composition. To the best of our knowledge, this is the first study to integrate clinical profiling, BA metabolomics, GM analysis, and mechanistic evaluation of a specific BA derivative in the context of DKD, thereby providing novel insights into endogenous BA-based renoprotection and potential therapeutic strategies.

# Methods and Materials

## Patients

This prospective cohort study was conducted at the Third Affiliated Hospital of Soochow University between April 2021 and August 2022, enrolling 92 consecutively recruited participants with type 2 diabetes mellitus (T2DM) and 31 age- and sex-matched healthy controls (HC). Inclusion criteria: (1) meeting the American Diabetes Association classification criteria for T2DM-2020;[11] (2) age > 18 years old. (3) estimated glomerular filtration rate (eGFR) ≥ 90 mL/min/1.73m$^2$ (CKD-EPI Creatinine).[12] Exclusion criteria: (1) presence of malignancy or pregnancy; (2) primary or secondary kidney diseases caused by other causes; (3) presence of liver or intestinal inflammatory diseases.

HC participants were enrolled based on the following inclusion criteria: (1) no known history of chronic systemic diseases (such as DM and hypertension); (2) no chronic systemic diseases requiring long-term medical treatment; (3) biochemical evidence of normal serum glucose levels, liver function, and kidney function.

The participants with T2DM were categorized into three groups according to their urine albumin-to-creatinine ratio (UACR): (1) T2DM with normoalbuminuria group (T2DM group, UACR < 30mg/g, n = 31); (2) clinically diagnosed DKD[13] with microalbuminuria group (DKD micro group, 30 ≤ UACR ≤ 300mg/g, n = 30); (3) clinically diagnosed DKD with macroalbuminuria group (DKD macro group, UACR > 300mg/g, n = 31). Additionally, to avoid interference from metabolite excretion, only participants with normal renal function (eGFR ≥ 90 mL/min/1.73m$^2$) were included in the study.

The study was conducted in accordance with the principles of the Declaration of Helsinki and was approved by the Third Affiliated Hospital of Ethics Committee of Soochow University (Ethics No: 2021–136, Approval date: 2021–03-10). Informed written consent was secured from all participants.

## Sample Collection

After overnight fasting, we collected fasting blood samples (5mL) from each participant and stored them in specimen tubes with EDTA as an anticoagulant. The blood samples were centrifuged at 4000 rpm for 15 minutes. The plasma specimens were then stored at −80°C.

## Animal Model

Thirty-one 4-week-old male C57 BL/6J mice were obtained from the Model Animal Research Center of Nanjing University (Nanjing, China). Mice were randomly assigned to experimental groups, and all procedures involving animals were conducted in accordance with institutional guidelines for the care and use of laboratory animals approved by the Ethics Committee of the Third Affiliated Hospital of Soochow University. The mice were housed under standard conditions, including a temperature of 24°C, humidity between 40−70%, and a 12-hour light/dark cycle with adequate air exchange. The mice were then randomly divided into 2 groups: a 10% low fat diet (LFD, n = 5) group; a 60% high fat diet (HFD, n = 26) group. At 14 weeks of age, 26 mice fed HFD were administered 40 mg/kg streptozotocin (STZ) via intraperitoneal injection daily for 5 consecutive days, while 5 mice from the LFD group received daily intraperitoneal injections of sodium citrate buffer for 5 consecutive days. The diabetic model was confirmed by fasting blood glucose (FBG) levels higher than 11.1 mmol/L. At 18 weeks of age, after overnight fasting, mice from the control group were gavaged with CMC-Na for 2 weeks, and mice from the diabetic group were gavaged with DHLCA 5 mg/kg (n = 5), 10 mg/kg (n = 8), 20 mg/kg (n = 5) (DKD-DHLCA group) or CMC-Na (n = 8, DKD group) for 2 weeks. All mice at 20 weeks of age were euthanized, and samples were harvested for further analysis. Urine creatinine (measured using a Hitachi automatic analyzer 3500) and urine albumin (measured using MedicalSystem) were determined according to standard laboratory methods. Biochemical indicators including blood urea nitrogen (BUN), serum creatinine (Scr), urine

creatinine, alanine aminotransferase (ALT), aspartate aminotransferase (AST), and total BA (TBA), were measured using an automated analyzer (Hitachi) following standard laboratory procedures.

## RNA Extraction and Real-Time Quantitative Polymerase Chain Reaction (RT-qPCR)

Total RNA was extracted from kidney tissues using Trizol reagent (Invitrogen, USA). The isolated RNA was then reverse-transcribed into cDNA using the PrimeScript™ RT reagent Kit (Takara, Japan) according to the manufacturer's instructions. RT-qPCR was performed using SYBR Premix Ex Taq™ (Takara, Japan) on a Thermo Fisher Scientific equipment. The specific mouse primer sequences (RiboBio, China) used are provided in Table 1. The expression of $\beta$-actin was used as an internal control.

## Western Blot (WB)

Kidney protein was extracted using radioimmunoprecipitation assay (RIPA) lysis buffer and the total protein concentration was quantified using a bicinchoninic acid (BCA) protein assay. The samples were then subjected to WB analysis.

**Table 1** Demographic and Clinical Characteristics of Participants

| Group | HC (n=31) | T2DM (n=31) | DKD Micro (n=30) | DKD Macro (n=31) | *P* value | FDR-q |
|---|---|---|---|---|---|---|
| Age (years) | 50.0 (41.0, 59.00) | 54.0 (47.0, 61.0) | 51.5 (37.8, 70.0) | 56.0 (51.0, 69.0) | 0.156 | 0.189 |
| Male/female (n) | 12/19 | 17/14 | 17/13 | 22/9 | 0.088 | 0.088 |
| Duration of DM (years) | – | 4.0 (0.5, 10.0) | 6.5 (1.0 11.3) | 10.0 (8.0, 15.0)$^{\#,\dagger}$ | <0.001 | 0.002 |
| BMI (kg/m$^2$) | – | 23.2 (21.4, 25.3) | 25.9 (23.4, 29.0)$^{\#}$ | 24.7 (22.3, 25.8) | 0.007 | 0.018 |
| WBC (10^9 g/L) | 5.2 (4.7, 6.2) | 5.7 (5.0, 6.7) | 6.3 (5.4, 7.9)* | 7.2 (5.8, 9.1)$^{*,\#}$ | <0.001 | 0.001 |
| RBC (10^12 g/L) | 4.6 (4.4, 4.8) | 4.6 (4.3, 4.8) | 4.6 (4.4, 5.2) | 4.2 (3.7, 4.7)$^{*,\#,\dagger}$ | 0.007 | 0.013 |
| Hb (g/L) | 138.0 (131.0, 145.0) | 138.0 (125.0, 145.0) | 139.5 (129.0, 153.3) | 121.0 (111.0, 140.0)$^{*,\dagger}$ | 0.008 | 0.014 |
| NLR | 1.8 (1.4, 2.3) | 1.6 (1.3, 2.0) | 1.7 (1.4, 2.1) | 2.4 (1.7, 4.4)$^{*,\#,\dagger}$ | <0.001 | 0.002 |
| ALB (g/L) | 44.9 (43.6, 46.4) | 39.1 (37.5, 42.5)* | 38.6 (36.9, 41.2)* | 35.2 (32.1, 38.8)$^{*,\#,\dagger}$ | <0.001 | <0.001 |
| BUN (mmol/L) | 5.1 ± 1.3 | 5.1 ± 1.5 | 5.8 ± 1.9 | 5.6 ± 1.8 | 0.249 | 0.249 |
| Scr (μmol/L) | 63.1 ± 9.8 | 56.7 ± 10.5* | 62.9 ± 8.3$^{\#}$ | 65.2 ± 10.4$^{\#}$ | 0.006 | 0.009 |
| eGFR (mL/min/1.73m$^2$) | 102.6 (94.9, 111.8) | 112.5 (103.4, 133.2)* | 110.8 (91.3, 121.2) | 97.7 (93.9, 105.0)$^{\#,\dagger}$ | <0.001 | 0.001 |
| Urine albumin (mg/L) | 13.3 (9.4, 21.8) | 12.1 (8.3, 14.9) | 68.7 (29.3, 133.8)$^{*,\#}$ | 667.1 (450.4, 1235.0)$^{*,\#,\dagger}$ | <0.001 | <0.001 |
| UACR (mg/g) | 9.7 (7.1, 10.6) | 10.7 (7.8, 19.2) | 84.0 (40.3, 154.1)$^{*,\#}$ | 928.1 (520.0, 1426.6)$^{*,\#,\dagger}$ | <0.001 | <0.001 |
| TC (mmol/L) | 4.6 (3.9, 5.3) | 4.9 (3.8, 5.4) | 5.0 (3.9, 5.6) | 4.4 (3.5, 5.6) | 0.776 | 0.851 |
| TG (mmol/L) | 1.0 (0.8, 1.5) | 1.3 (1.1, 2.5)* | 2.2 (1.5, 3.3)* | 1.7 (1.1, 2.7)* | <0.001 | <0.001 |
| HDL (mmol/L) | 1.5 (1.2, 1.7) | 1.1 (1.0, 1.3)* | 1.0 (0.8, 1.1)*$^{\#}$ | 1.0 (0.8, 1.2)* | <0.001 | <0.001 |
| LDL (mmol/L) | 2.6 (2.1, 3.1) | 2.7 (1.8, 3.1) | 2.5 (2.1, 3.2) | 2.5 (2.0, 3.0) | 0.893 | 0.907 |
| HbA1c (%) | – | 8.2 (7.8, 10.5) | 9.0 (7.3, 11.0) | 10.4 (8.2, 11.9) | 0.226 | 0.226 |
| FBG (mmol/L) | 5.0 ± 0.4 | 9.1 ± 3.4* | 10.1 ± 3.5* | 10.8 ± 4.3* | <0.001 | <0.001 |
| FCP (ng/mL) | – | 498.7 (346.4, 560.0) | 661.5 (529.2, 837.3)$^{\#}$ | 486.7 (345.8, 743.2) | 0.009 | 0.018 |
| ALT (U/L) | 17.7 (15.0, 22.3) | 19.1 (14.3, 23.1) | 21.5 (13.4, 68.8) | 17.4 (11.6, 29.2) | 0.529 | 0.591 |
| AST (U/L) | 23.1 (18.6, 27.1) | 17.6 (14.7, 22.0) | 20.7 (14.4, 40.0) | 16.2 (14.3, 26.2) | 0.050 | 0.073 |
| GGT (U/L) | 18.7 (14.4, 29.4) | 22.7 (14.6, 28.5) | 31.3 (16.8, 59.2)* | 22.2 (18.1, 37.5) | 0.029 | 0.044 |
| ALP (U/L) | 75.0 (63.0, 97.0) | 73.0 (65.0, 89.0) | 79.0 (68.0, 98.0) | 97.0 (69.0, 118.0) | 0.126 | 0.163 |
| LDH (U/L) | – | 143.0 (135.0, 162.0) | 171.0 (155.0, 204.3)$^{\#}$ | 175.0 (153.0, 196.0)$^{\#}$ | <0.001 | 0.002 |
| ADA (U/L) | – | 12.4 (10.3, 15.1) | 14.5 (11.8, 19.0) | 15.9 (12.6, 22.4)$^{\#}$ | 0.014 | 0.023 |
| CHE (U/L) | – | 8850.0 (7221.0, 10,548.0) | 9179.0 (7419.3, 11,101.8) | 7301.0 (5967.0, 10,088.0) | 0.069 | 0.083 |
| TBA (mmol/L) | – | 3.7 (2.3, 6.6) | 4.7 (2.6, 7.8) | 2.8 (1.6, 5.8) | 0.073 | 0.083 |
| TBIL (mmol/L) | 13.3 (9.7, 17.8) | 12.6 (9.0, 15.0) | 12.9 (10.7, 14.0) | 9.2 (7.3, 11.9)$^{*,\#,\dagger}$ | 0.002 | 0.005 |
| DBIL (mmol/L) | 4.4 (2.9, 5.2) | 3.9 (2.9, 4.6) | 3.8 (3.2, 5.0) | 3.0 (2.5, 4.4) | 0.083 | 0.112 |
| IBIL (mmol/L) | 9.3 (6.8, 12.6) | 8.5 (6.1, 10.6) | 8.5 (6.9, 9.8) | 5.9 (4.7, 6.6)$^{*,\#,\dagger}$ | <0.001 | 0.001 |

**Notes**: *FDR-q < 0.05 (compared to HC group); $^{\#}$FDR-q < 0.05 (compared to T2DM group); $^{\dagger}$FDR-q < 0.05 (compared to DKD micro group).
**Abbreviations**: HC, healthy control; DM, diabetes mellitus; DKD, diabetic kidney disease; FDR, false discovery rate; BMI, body mass index; WBC, white blood cell; RBC, red blood cell; Hb, haemoglobin; NLR, neutrophil to lymphocyte ratio; ALB, albumin; BUN, blood urea nitrogen; Scr, serum creatinine; eGFR, estimated glomerular filtration rate; UACR, urine albumin-to-creatinine ratio; TC, total cholesterol; TG, triglycerides; HDL, high-density lipoprotein; LDL, low-density lipoprotein; HbA1c, hemoglobin A1c; FBG, fasting blood glucose; FCP, fasting c-peptide; ALT, alanine aminotransferase; AST, aspartate aminotransferase; GGT, gamma-glutamyl transferase; ALP, alkaline phosphatase; LDH, lactate dehydrogenase; ADA, adenosine deaminase; CHE, cholinesterase; TBA, total bile acid; TBIL, total bilirubin; DBIL, direct bilirubin; IBIL, indirect bilirubin.

Prior to incubation with primary antibodies against TGR5 (ab72608, Abcam, USA), FXR (sc-25309, Santa Cruz, USA), and $\beta$-actin (MA1-140, Invitrogen, USA) overnight at 4°C, the nitrocellulose membranes were blocked with 5% bovine serum albumin (BSA) to prevent non-specific binding. Quantitative analysis was performed using the Image J program. The protein levels were normalized against $\beta$-actin.

## Histology, Immunohistochemical and Immunofluorescence Staining

Kidney tissue samples were fixed in 4% formaldehyde for 48 hours, dehydrated, and embedded in paraffin. Thin sections (4 μm thickness) were cut and stained with hematoxylin-eosin (H&E), periodic acid-Schiff (PAS), and Masson's trichrome stains. For immunohistochemical staining, antigen retrieval was performed in a nitrate solution at 96°C for 10 minutes. The tissue sections were blocked with 3% bovine serum albumin (BSA) for 30 minutes at room temperature, followed by overnight incubation at 4°C with primary antibodies against TGR5 and FXR. The slides were then incubated with appropriate secondary antibodies, washed, and developed using 3,3'-diaminobenzidine chromogen (Servicebio, China).

The severity of tubulointerstitial injury was evaluated based on an interstitial fibrosis and tubular atrophy (IFTA) scoring system. The IFTA score was defined as the percentage of the total involved area of interstitium and tubules, where 0 = no IFTA; 1 = less than 25% IFTA; 2 = 25% ~ 50% IFTA; 3 = at least 50% IFTA.[14] Histological assessments were performed by investigators who were blinded to group assignments to minimize observational bias.

## Plasma Metabolite Analysis

Plasma BAs profiling metabolites were analyzed using ultrahigh-performance liquid chromatography tandem-mass spectrometry (UPLC-MS/MS) platform, employing a widely targeted metabolomics analysis. The sample preparation and extraction procedures were as follows: Samples stored at −80°C were thawed on ice. Then, 50 μL of the sample and 300 μL of an extraction solution (1:1 acetonitrile: methanol, containing internal standards) were added to a 2 mL microcentrifuge tube. The mixture was vortexed for 3 minutes and centrifuged at 12,000 rpm for 15 minutes at 4°C. The 200 μL supernatant was collected, incubated at −20°C for 1 hour to precipitate proteins, and 180 μL aliquots were transferred for UPLC-MS/MS analysis.

## Metagenomic Sequencing and Analysis

Fecal DNA was extracted from mice using the FastDNA SPIN Kit (MP Biomedicals, USA). DNA quantity and quality were assessed with the Qubit™ dsDNA Quantification Assay Kits (Invitrogen, USA). Libraries were prepared from 200 ng input DNA using the TruSeq DNA Nano (Illumina) and sequenced on the Illumina NovaSeq 6000 platform (paired-end). Raw reads were trimmed for adaptors and low-quality bases using Cutadapt and Fqtrim, and host contamination was removed using Bowtie2. Clean reads were assembled using MEGAHIT, followed by gene prediction and redundancy removal to generate a non-redundant gene catalog. Taxonomic annotation was performed by aligning predicted proteins to the NCBI NR database using DIAMOND. Differential microbial taxa were identified using linear discriminant analysis effect size (LEfSe) (linear discriminant analysis [LDA] score > 3, $P < 0.05$).

## Data and Statistical Analysis

Data processing and statistical analyses were performed using R (v4.5.0; R Core Team, 2025), SPSS (v25.0; IBM Corp., Armonk, NY, USA, 2017), and GraphPad Prism (v9.0; GraphPad Software, San Diego, CA, USA, 2022). The normality of continuous variables was assessed using the Kolmogorov–Smirnov test. Categorical variables were summarized as counts. Normally distributed data were expressed as mean ± standard deviation (SD), while non-normally distributed data were reported as median (interquartile range, IQR). Multiple-group comparisons were performed using one-way ANOVA (parametric) or the Kruskal–Wallis $H$-test (non-parametric). When overall differences were significant ($P < 0.05$), post hoc pairwise comparisons were conducted using Tukey's test (ANOVA) or Dunn's test (Kruskal–Wallis). False discovery rate (FDR) correction was applied for multiple testing in omics-level comparisons (BAs and GM analyses). Categorical variables were compared using the chi-square test with FDR correction for multiple group comparisons. Dose–response curves for FBG and UACR were plotted using nonlinear regression (GraphPad Prism) from median ± SD values. For RT-qPCR and WB analyses (n = 3 per group), one-way ANOVA with bootstrap resampling (1000 iterations) was used to

estimate bias-corrected and accelerated 95% CI, followed by Tukey's post hoc test for multiple comparisons. Partial Spearman correlation coefficients were calculated to examine the association between clinical indicators and BA concentrations in patients, with adjustment for age and diabetes duration; two-sided *P* values were corrected for multiple testing with the FDR correction, and 95% confidence intervals were generated from 1000 bootstrap replicates. Receiver operating characteristic (ROC) curve analysis was used to assess diagnostic performance with area under the curve (AUC). Two-sided *P* values or FDR-q values < 0.05 were considered statistically significant.

# Results

## Alterations in the Plasma Levels of BAs in Patients with DKD

To investigate the alterations in the plasma levels of BAs in patients with DKD, UPLC-MS/MS was used to detect plasma BAs metabolic profiling. Baseline clinical characteristics of participants were compared among the groups (Table 1). The DKD macro group exhibited higher urine albumin, UACR, and neutrophil to lymphocyte ratio (NLR), but lower serum albumin (ALB), red blood cell (RBC), total bilirubin (TBIL), and indirect bilirubin (IBIL) compared to the other three groups ($P < 0.05$, Table 1).

A total of 50 BAs were detected. Furthermore, MetaboAnalyst was utilized to normalize, process, analyze, and interpret the metabolomic data. The differential metabolites between groups were visualized as a heat map (Figure 1). Plasma concentrations of five primary BAs (nor cholic acid [NCA], cholic acid [CA], glycochenodeoxycholic acid-3-sulfate [GCDCA-3S], chenodeoxycholic acid-3-$\beta$-D-glucuronide [CDCA-3Gln], and glycochenodeoxyche olic acid-3-O-$\beta$-glucuronide [GCDCA-3Gln]) and six secondary BAs (DHLCA, lithocholic acid [LCA], deoxycholic acid [DCA], 3-dehydrocholic acid [3DHCA], glycolithocholic acid [GLCA], and taurolithocholic acid [TLCA]) differed significantly among the four groups—HC, T2DM, DKD micro or DKD macro—with FDR-q values < 0.05. Variations in metabolite levels across groups are presented as box plots (Figure 2A and B).

## Partial Spearman Correlations Between Clinical Indicators and BAs

Partial Spearman correlation analysis, adjusted for age and diabetes duration, was performed between 11 differentially expressed bile acids and clinical indicators, with FDR correction applied for multiple testing (Figure 3). Notably, three secondary BAs—DHLCA, TLCA, and GLCA—showed significant inverse correlations with urinary albumin excretion. Plasma levels of DHLCA were negatively correlated with both urine albumin ($\rho = -0.347$; 95% CI, –0.531 to –0.135; $q = 0.008$) and the UACR ($\rho = -0.332$; 95% CI, –0.499 to –0.155; $q = 0.010$). Similarly, TLCA exhibited strong negative correlations with urine albumin ($\rho = -0.416$; 95% CI, –0.563 to –0.250; $q = 0.001$) and UACR ($\rho = -0.374$; 95% CI, –0.554 to –0.188; $q = 0.003$). GLCA also correlated inversely with urine albumin ($\rho = -0.324$; 95% CI, –0.520 to –0.114; $q = 0.012$) and UACR ($\rho = -0.329$; 95% CI, –0.533 to –0.125; $q = 0.011$). The full set of adjusted correlation coefficients, 95% CI, and FDR-q values of is presented in Table S1. These results suggest that lower circulating levels of specific secondary BAs are associated with higher degrees of albuminuria in patients with DKD.

## Diagnostic Values of DHLCA for Albuminuria

ROC curve analysis was performed to evaluate the diagnostic performance of plasma DHLCA in distinguishing macroalbuminuria from microalbuminuria in patients with DKD. DHLCA yielded an AUC of 0.738 (95% CI, 0.609 to 0.867), indicating moderate discriminative ability (Figure 4).

## Effects of DHLCA Intervention on DKD

To assess the effects of DHLCA on DKD, STZ-induced mice received 5, 10, or 20 mg/kg DHLCA. After 20 weeks, the 10 mg/kg group showed the greatest improvements in kidney function and glucose metabolism, as reflected by reduced UACR (Figure S1A), FBG (Figure S1B), IFTA (Figure S1C and D), and tubular injury markers (kidney injury molecule-1 [KIM-1], neutrophil gelatinase-associated lipocalin [NGAL]; Figure S1E). Dose–response analysis revealed that therapeutic benefits increased up to 10 mg/kg and plateaued thereafter (Figure S2). Therefore, 10 mg/kg was selected

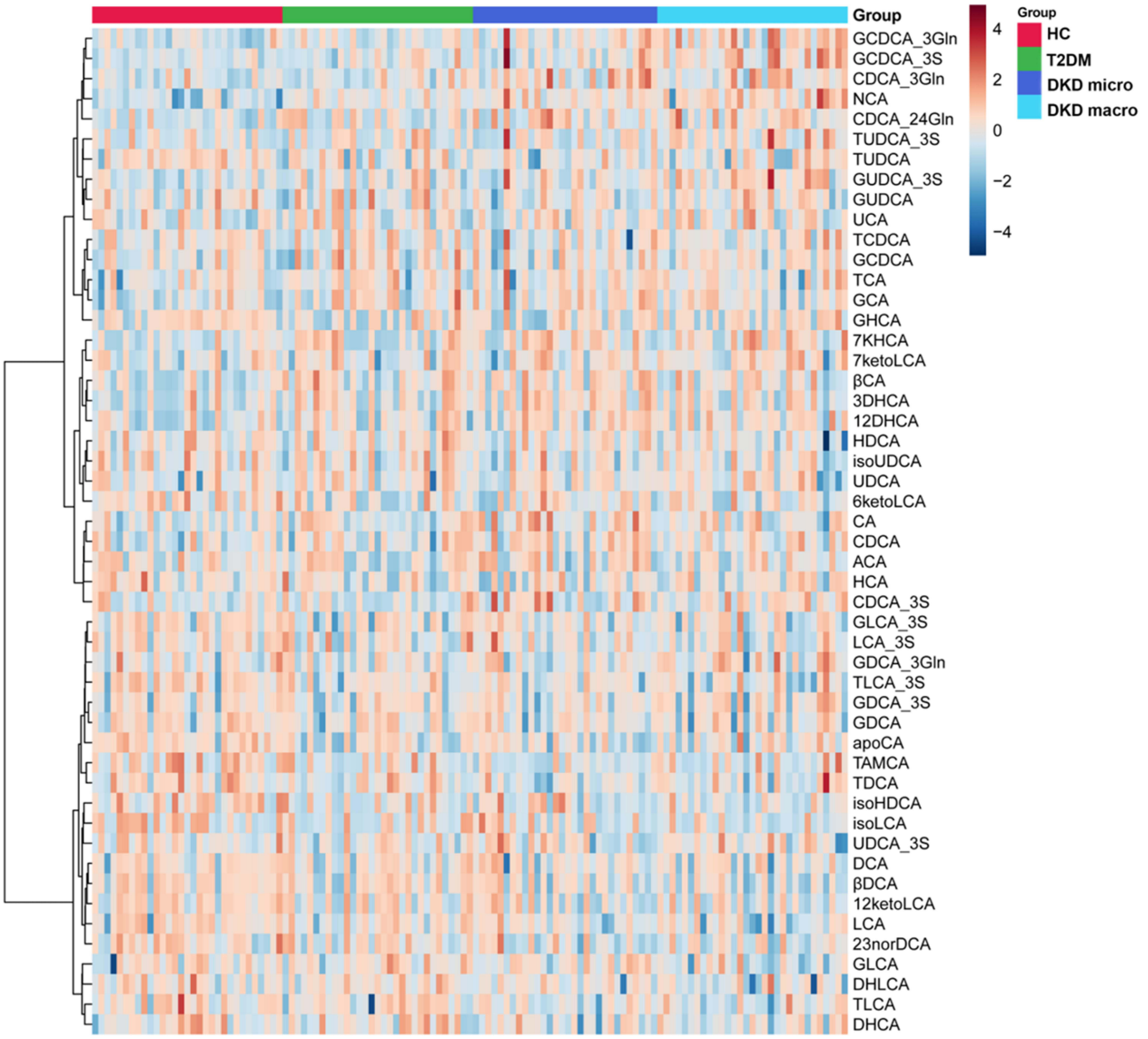


**Figure 1** Metabolite heat map in the four groups. Samples are represented in the columns, metabolites are represented in the rows, and their relative concentrations are displayed by color. Metabolites between the groups of participants who are HC group, T2DM group, DKD micro group, and DKD macro group are displayed on the heat map.

for subsequent evaluation. Representative comparisons among the control, DKD, and 10 mg/kg DHLCA-treated DKD groups are shown in Figure 5.

Compared to the DKD group, UACR, kidney weight/body weight ratio, TBA, and FBG (20W) in the DKD+DHLCA group were significantly reduced ($P < 0.05$, Figure 6A and H). However, DHLCA treatment did not impact creatinine clearance rate (Ccr) and BUN ($P > 0.05$, Figure 6B and C).

In terms of liver indexes, the DKD group demonstrated significantly elevated ALT and AST levels compared to the control group ($P < 0.05$, Figure 6E and F). The DKD+DHLCA group showed a significant decrease in ALT levels compared to the DKD group ($P < 0.05$, Figure 6E), indicating DHLCA's potential to improve liver function.

H&E, PAS and Masson staining images illustrated that DHLCA alleviate renal tubular injury in DKD mice. IFTA score was decreased in the DKD+DHLCA group compared with the DKD group ($P < 0.05$, Figure 7A and B). The expressions of KIM-1 and NGAL were also reduced in the DKD+DHLCA group compared to the DKD group (Figure 7C). Furthermore, immunohistochemistry and immunofluorescence of the kidney showed the expressions


https://doi.org/10.2147/DDDT.S530823

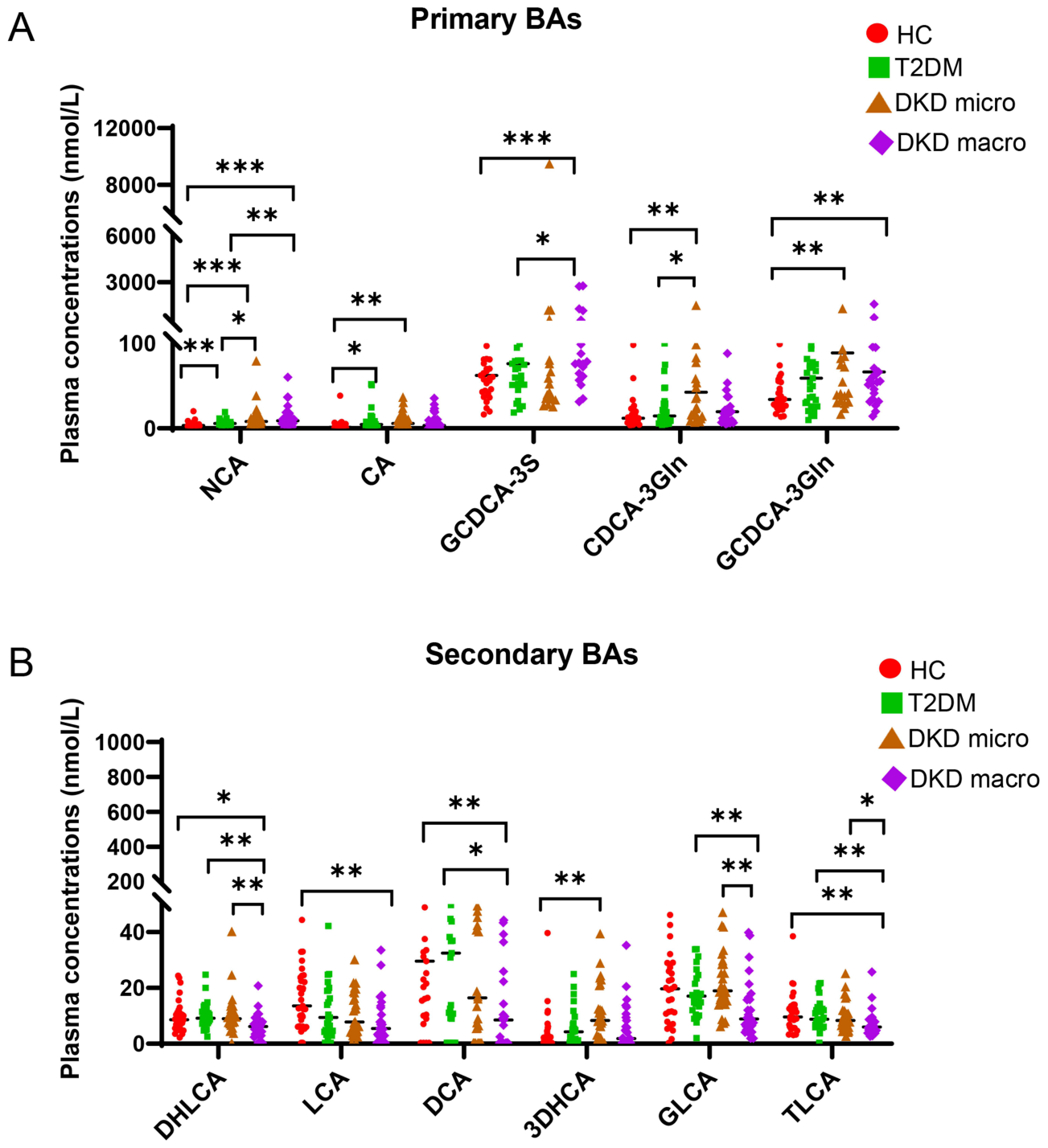


**Figure 2** BA profiles among different groups. (**A**) Plasma primary BAs. (**B**) Plasma secondary BAs. *FDR-q < 0.05; **FDR-q < 0.01; ***FDR-q < 0.001.

TGR5 and FXR in renal tubular epithelial cells were significantly upregulated following DHLCA treatment (Figure 7E). The mRNA and protein expressions of TGR5 and FXR in the DKD+DHLCA group were also higher than the DKD group ($P < 0.05$, Figure 7D, and G, Table 2).

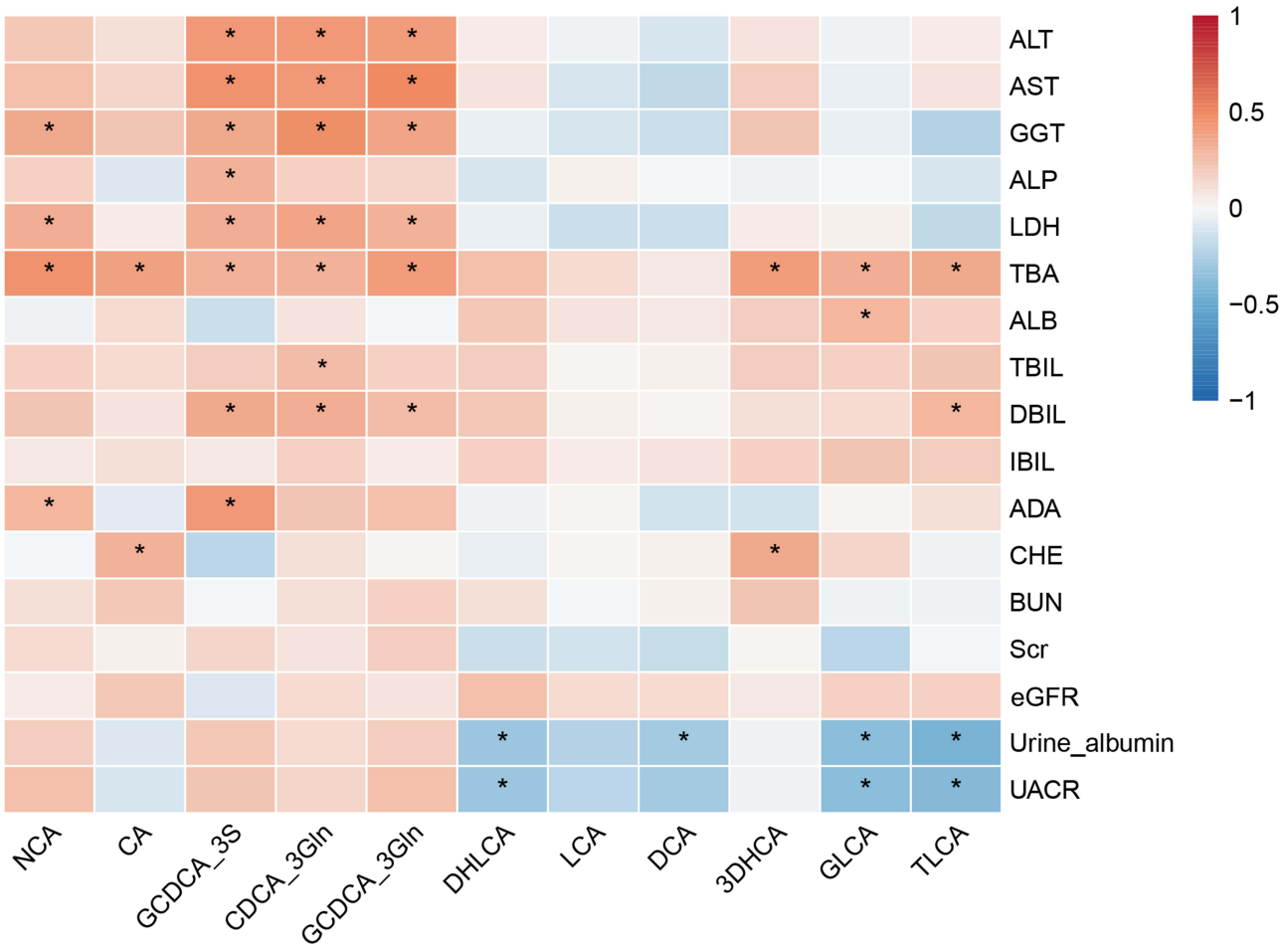


**Figure 3** Correlations between clinical indicators and BAs metabolites. *FDR-q < 0.05.

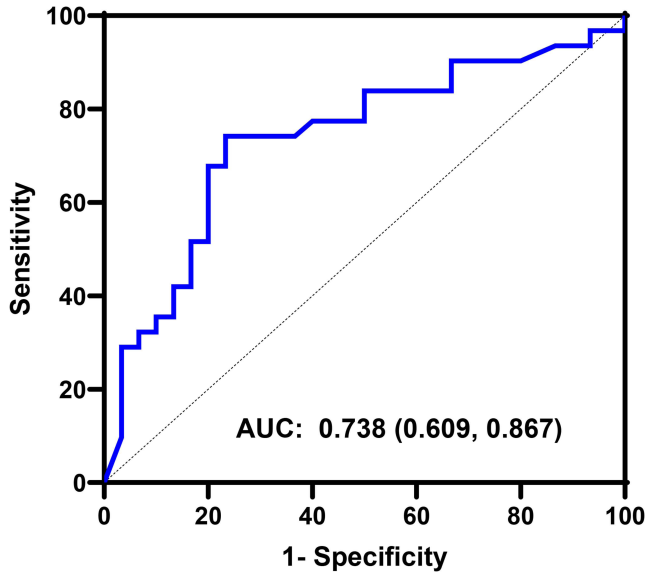


**Figure 4** ROC curve of DHLCA on DKD with macroalbuminuria.


https://doi.org/10.2147/DDDT.S530823

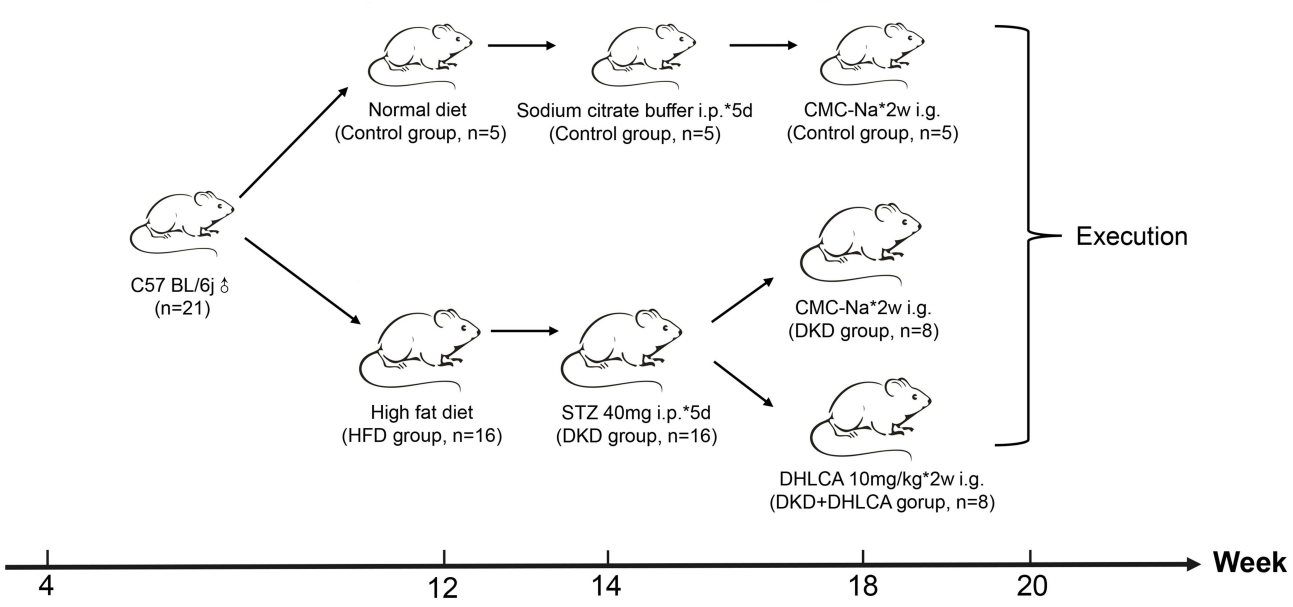


**Figure 5** DHLCA treatment on DKD mice models.

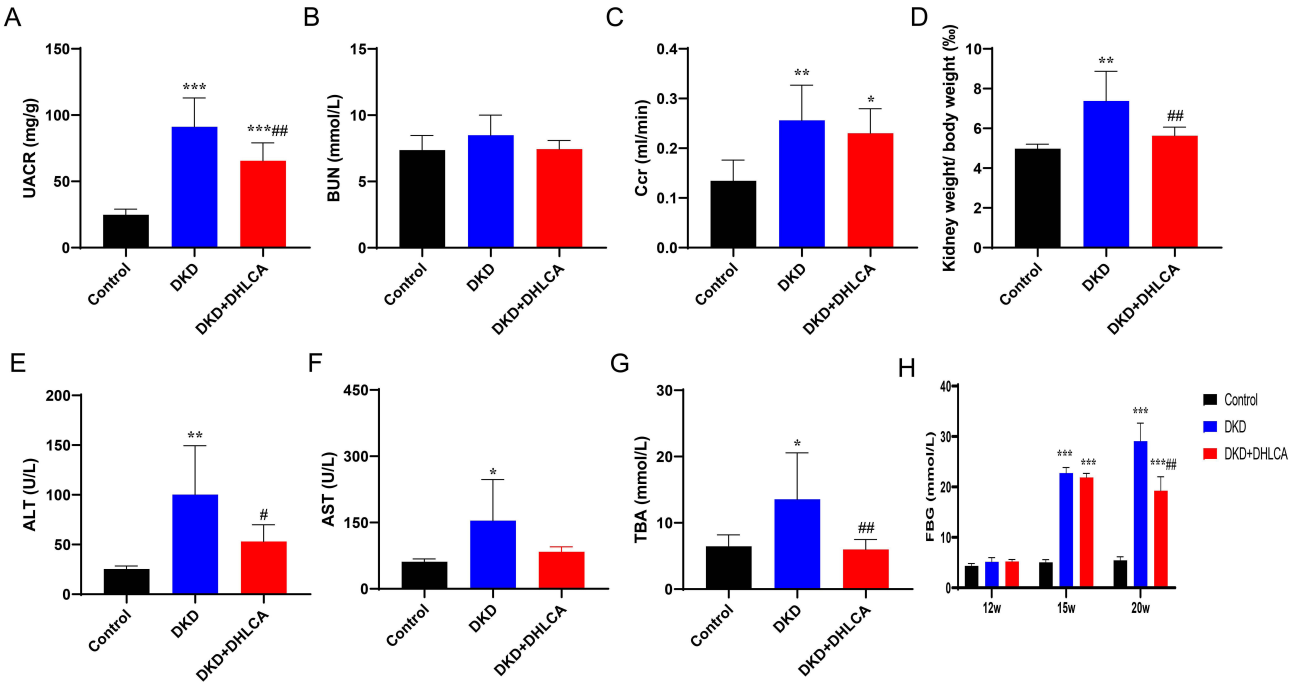


**Figure 6** DHLCA alters kidney and liver indices in DKD mice. (**A**) UACR. (**B**) BUN. (**C**) Ccr. (**D**) Kidney weight/body weight. (**E**) ALT. (**F**) AST. (**G**) TBA. (**H**) FBG. $^{*}P < 0.05$ (compared to Control group); $^{**}P < 0.01$ (compared to Control group); $^{***}P < 0.001$ (compared to Control group); $^{\#}P < 0.05$ (compared to DKD group); $^{\#\#}P < 0.01$ (compared to DKD group).

## The Impact of DHLCA Treatment on the GM Composition of DKD Mice

To explore the specific GM involved in DHLCA treatment on DKD, we conducted metagenomic analysis on GM of DKD and DKD+DHLCA mice. The phylogenetic tree showed the changes in the composition of GM at the seven levels (domain, phylum, class, order, family, genus, and species) (Figure 8A). The bar graph displayed the differential GM with LDA score > 3 and $P < 0.05$ (Figure 8B). According to the LEFSe analysis, a total of 17 different species were identified. As shown in Figure 8C, the DKD+DHLCA group exhibited an increase in *Lachnospiraceae bacterium* (*Lachnospiraceae*

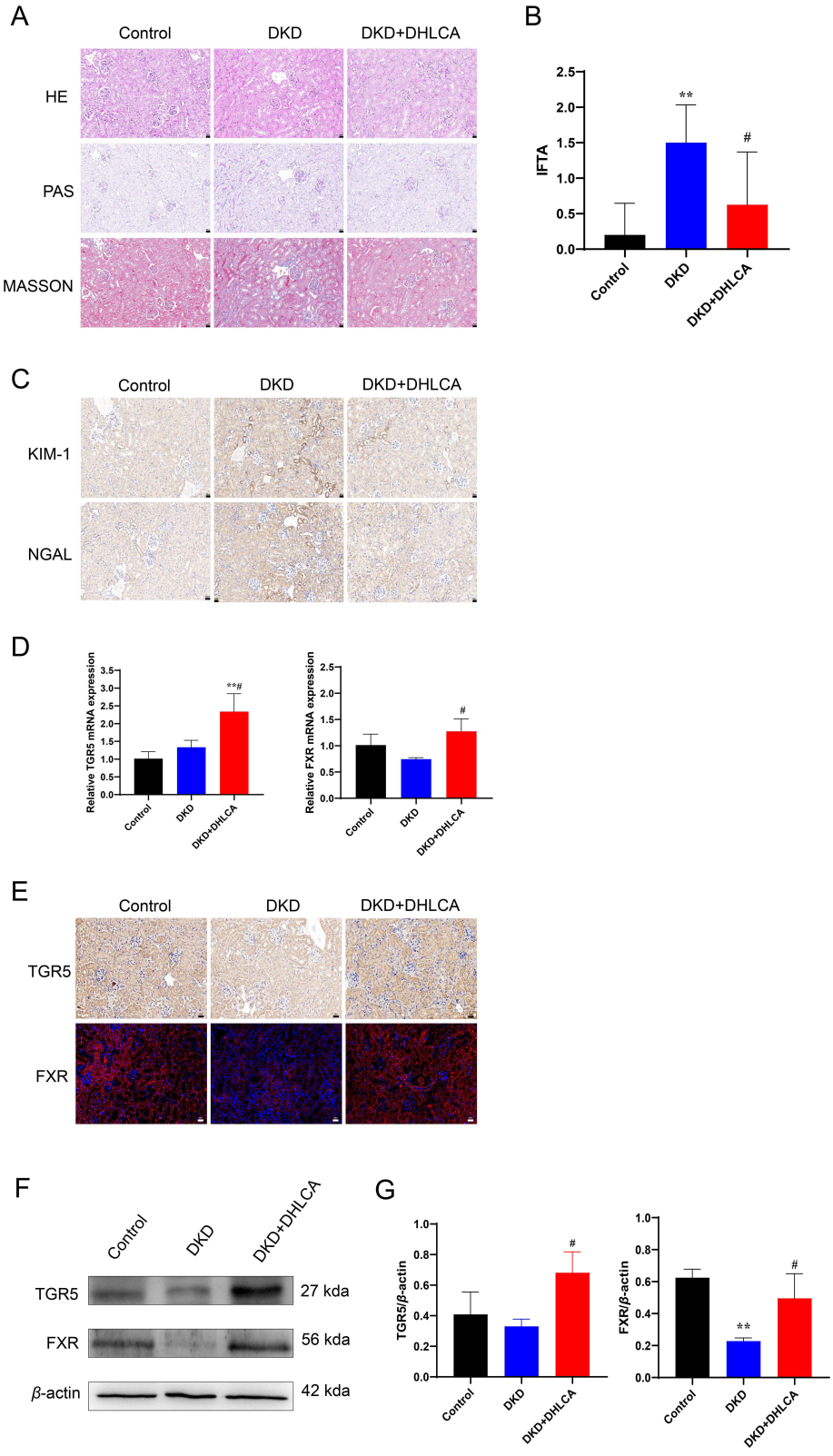


**Figure 7** DHLCA alleviates renal tubular injury in DKD mice. (**A**) Morphological examinations of renal pathology by H&E, PAS, Masson staining (Magnification 40×, Control group: n = 5, DKD group: n = 8, DKD+DHLCA group: n = 8). (**B**) Quantification of IFTA score of the kidneys in each group (Magnification 40×, Control group: n = 5, DKD group: n = 8, DKD+DHLCA group: n = 8). (**C**) Immunohistochemistry staining for KIM-1 and NGAL (Magnification 40×, Control group: n = 5, DKD group: n = 8, DKD +DHLCA group: n = 8). (**D**) The gene expressions of TGR5 and FXR by RT-qPCR (n = 3). (**E**) Immunohistochemistry staining for TGR5 and immunofluorescence staining for FXR (Magnification 40×, Control group: n = 5, DKD group: n = 8, DKD+DHLCA group: n = 8). (**F**) The protein expressions TGR5 and FXR by WB (n = 3). (**G**) Quantitative measurement of WB bands normalized to *β*-actin (n = 3). $^{**}P < 0.01$ (compared to Control group); $^{\#}P < 0.05$ (compared to DKD group).


https://doi.org/10.2147/DDDT.S530823

**Table 2** Sequences of the Primers

| Gene | Species | Forward Primer | Reverse Primer |
|---|---|---|---|
| *β-actin* | Mouse | 5'-TCAAGATCATTGCTCCTCCTGAG-3' | 5'-ACATCTGCTGGAAGGTGGACA-3' |
| *Tgr5* | Mouse | 5'-CTCTACCTGGAAGTTTATGGCCT-3' | 5'-AGTCGGCGGATCTCACACA-3' |
| *Fxr* | Mouse | 5'-TGTACCAGCCTGAGAACCCG-3' | 5'-TGTGATCATTCACTCTCCAAGACAT-3' |

*bacterium M18-1, Lachnospiraceae bacterium 3–1, Lachnospiraceae bacterium, Lachnospiraceae bacterium MD308, Lachnospiraceae bacterium 28–4, Acetatifactor muris), Bacteroides acidifaciens, Firmicutes* (*Firmicutes bacterium ASF500, Eubacterium sp. CAG:180*), *Bacterium 1xD42-87, Bacterium 1xD42-67, and Acutalibacter sp. 1XD8-33*, but a decrease in *Akkermansia muciniphila, Muribaculaceae unclassified, Bacteroidales unclassified, Bacteroidales bacterium, and Muribaculaceae bacterium Isolate-037 (Harlan)*.

## The Correlations Between BAs, GM and Biochemical Indicators

To investigate the relationship between host metabolic parameters and GM following DHLCA intervention, partial Spearman correlation analysis was performed between serum biochemical indicators and fecal microbial taxa, with FDR correction applied. Notable trends were observed between specific bacterial species and FBG as well as UACR. *Muribaculaceae bacterium Isolate-*

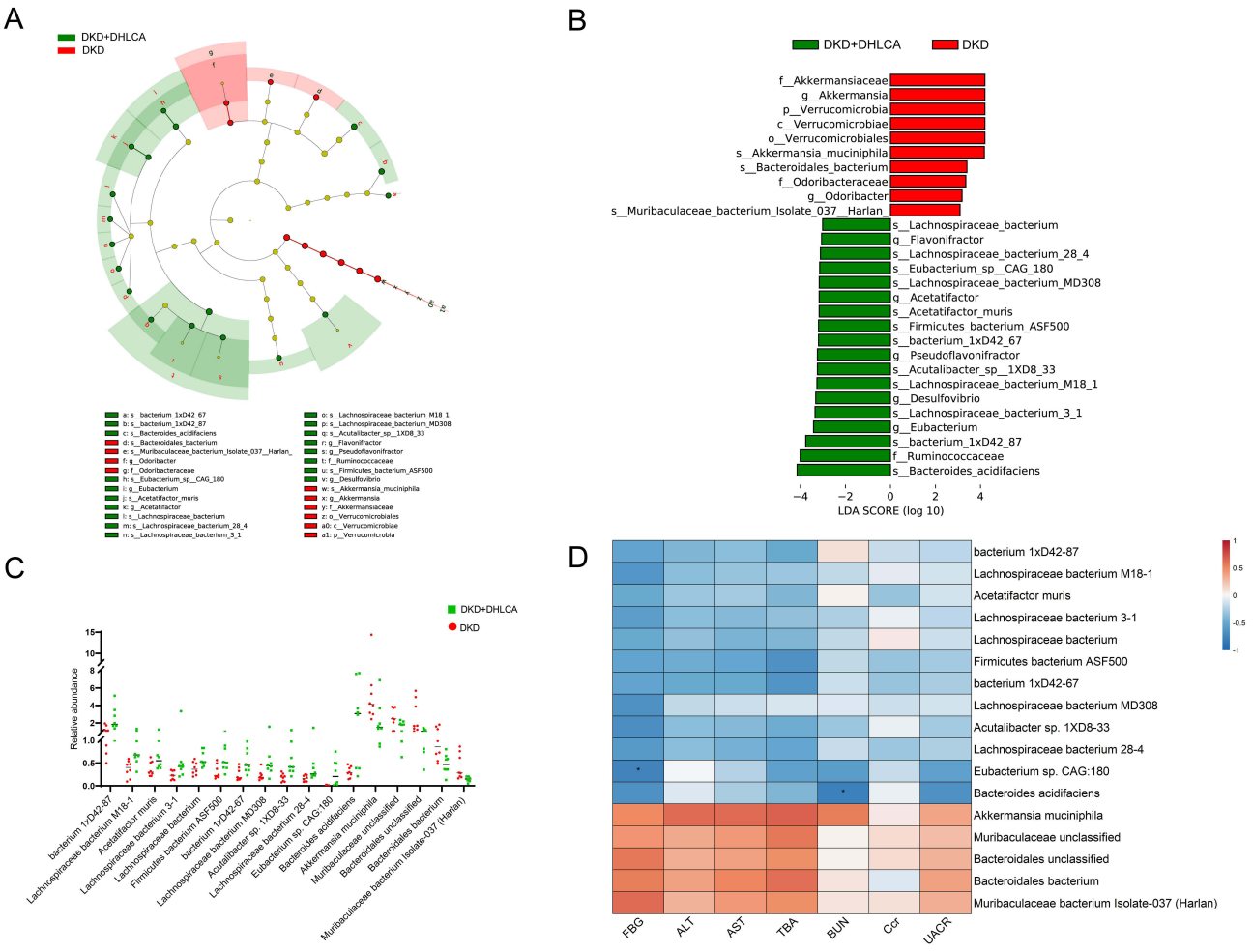


**Figure 8** DHLCA modulates the composition of GM. (**A**) The phylogenetic tree in mice between the DKD and DKD+DHLCA groups. (**B**) The bar graph displayed the differential GM with LDA scores > 3 and P < 0.05. (**C**) The differences of GM composition at species level in mice between the DKD and DKD+DHLCA groups. (**D**) Correlations between GM and biochemical indicators in mice. *FDR-q < 0.05.

*037 (Harlan)* and *Bacteroidales bacterium* showed the strong positive correlations with both FBG and UACR, suggesting a potential association with hyperglycemia and kidney injury. In contrast, *Eubacterium sp. CAG:180* and *Bacteroides acidifaciens* exhibited the strong negative correlations with FBG and UACR, indicating possible protective roles under DHLCA treatment (Figure 8D).

To evaluate the effects of DHLCA intervention on GM and fecal BA metabolism, we assessed the correlations between six major secondary BAs in feces and microbial taxa using Spearman correlation analysis with FDR correction. Notable correlation trends were observed between DHLCA levels and specific bacterial taxa. Among the analyzed taxa, *Lachnospiraceae bacterium MD308* and *Lachnospiraceae bacterium M18-1* showed the strong positive correlations with fecal DHLCA concentrations (Figure 9). Conversely, *Muribaculaceae bacterium Isolate-037 (Harlan)* exhibited the

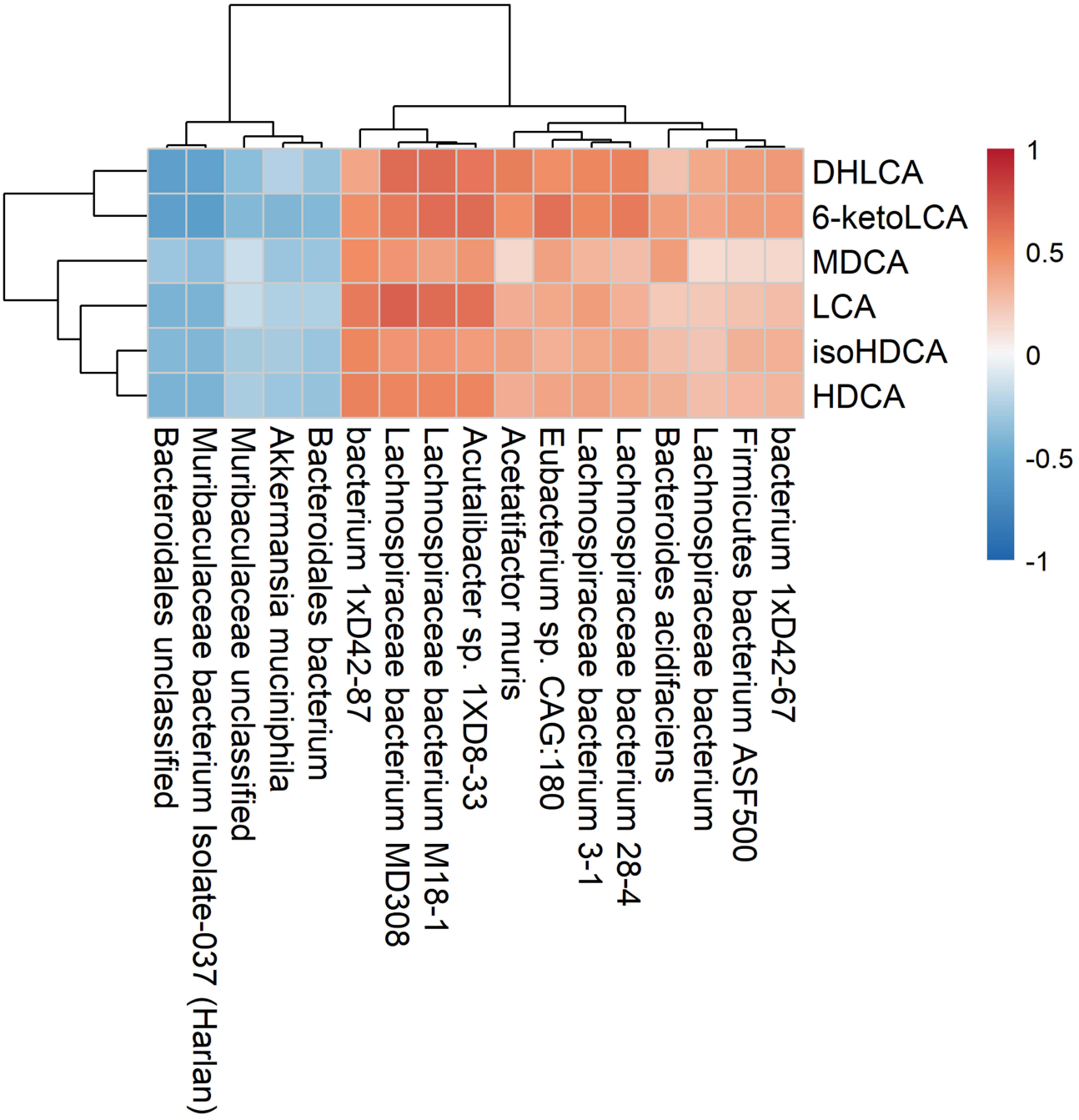


**Figure 9** Correlation analysis and hierarchical clustering heat map of GM and BAs.


https://doi.org/10.2147/DDDT.S530823

strong negative correlation (Figure 9), suggesting a potential antagonistic relationship with DHLCA metabolism or abundance. Although these associations did not reach statistical significance after FDR correction, the observed trends highlight candidate microbial taxa potentially involved in the gut metabolic response to DHLCA intervention.

## Discussion

DKD is a significant complication of diabetes and a leading cause of ESRD. Metabolism disruptions play a key role in initiating DKD.[15] Metabolomics can offer a unique metabolic profile of the disease, aiding in prediction and diagnosis.[16] While TGR5 and FXR have shown promise as treatment targets for nephropathy in diabetes and obesity, gaps remain in understanding the upstream pathway. Our present study indicated differential BA metabolism in various DKD stages. Plasma DHLCA levels were negatively correlated with albuminuria, and DHLCA intervention activated TGR5 and FXR, leading to improved tubular injury, UACR, FBG, and gut microbial changes in DKD mouse models.

Disruption of BA metabolism is a hallmark of DKD, and we found that plasma BA profiles shift in parallel with worsening albuminuria. Specifically, DHLCA fell in patients with macroalbuminuria and was inversely correlated with urinary albumin excretion, implicating loss of this metabolite in disease progression. In STZ-induced DKD mice, DHLCA restored kidney expression of the BA receptors TGR5 and FXR, improved tubular injury, and reduced the UACR, indicating that DHLCA exerts renoprotection primarily through concerted activation of these two receptors.

TGR5 and FXR can modulate glucose and lipid homeostasis, mitochondrial integrity, oxidative stress, and fibrogenesis; simultaneous stimulation therefore yields additive benefit. The synthetic dual agonist INT-767 ameliorates proteinuria and renal fibrosis in experimental DKD, underscoring the value of dual receptor engagement.[17] In metabolic disease models, TGR5 activation enhances glucose utilization and energy expenditure, whereas FXR activation normalizes BA turnover and suppresses inflammation—effects that translate into protection against obesity, diabetes, and DKD.[17–23] Taken together, our data identify DHLCA as an endogenous dual agonist that activates TGR5/FXR signaling, and counteracts key metabolic and inflammatory drivers of DKD progression.

Alterations in GM composition have been observed in the early stages of DKD,[24,25] and increasing evidence suggests a bidirectional regulatory relationship between BAs and GM.[26] Our study further explored the correlations between BAs and GM by analyzing fecal samples from the DKD group and the DKD+DHLCA group in mice. The results demonstrated that DHLCA can influence GM composition, with an increase in the abundance of *Lachnospiraceae bacterium* in the DKD+DHLCA group. *Lachnospiraceae*, known for producing short-chain fatty acid (SCFA) with immunoregulatory properties,[27] has been associated with conditions like DM[28] and DKD.[29] The upregulation of *Lachnospiraceae* after DHLCA intervention suggests that DHLCA may indirectly regulate GM to improve DKD. Our results also demonstrated a significant upregulation in the abundance of *Bacteroides acidifaciens* following DHLCA intervention. *Bacteroides acidifaciens* has been shown to play a protective role against obesity and enhance insulin sensitivity in murine models.[30] The impact of these GM changes on DKD after DHLCA intervention remains unclear. This question may be solved by isolating and transplanting a specific single bacterial strain in the future.

DM is a metabolic disorder involving impaired glucose and lipid metabolism, often leading to complications such as nonalcoholic fatty liver disease (NAFLD). Liver involvement in DM can elevate serum ALT and AST levels due to hepatic dysfunction.[31] Our findings reveal that DHLCA lowers serum ALT levels in DKD mice, suggesting a novel hepatoprotective role that has not been documented in prior studies. DHLCA, a bile acid derivative, has been shown to exert dual actions on metabolic and immune pathways. Specifically, it inhibits Th17 cell differentiation and suppresses IL-17A production,[32] thereby mitigating liver injury driven by immune-mediated inflammation.[33] Concurrently, DHLCA improves insulin sensitivity via activation of FXR and TGR5 signaling,[34,35] thereby decreasing hepatocellular injury caused by metabolic dysregulation. These combined effects likely contribute to hepatocellular protection and the observed decrease in serum ALT. Therefore, we hypothesized that, beyond its renoprotective effects in DKD, DHLCA may also confer benefits on liver function. Further experimental studies are warranted to validate this hypothesis and elucidate the underlying mechanisms.

The study presented has shed light on the potential therapeutic benefits of DHLCA in the context of DKD. However, it is important to acknowledge several limitations that were identified within the research. First, the sample size was limited, with only n = 3 biological replicates per group for the RT-qPCR and WB assays, and n = 122 in the clinical

cohort, restricting statistical power; the findings from molecular experiments should be considered preliminary and require further validation in larger cohorts. Second, the single-center Chinese cohort limits generalizability, and unmeasured variables—including diet, medications, and comorbidities—may have influenced BA profiles. Future multi-center studies with more rigorous control of confounding factors are needed to validate and extend these findings. Third, therapeutic efficacy was assessed at a single time point using surrogate markers of early DKD injury, rather than hard renal endpoints. Serial measurements and longer follow-up are warranted. Fourth, the study lacks in vitro evidence confirming DHLCA-mediated activation of TGR5 or FXR. Future in vitro studies are planned to validate DHLCA-induced activation of these receptors and to clarify its direct protective mechanisms on renal tubular epithelial cells. Fifth, the lack of species-level functional annotations restricts mechanistic insight into how specific microbial taxa contribute to BA and SCFA metabolism. The causal links among GM alterations, BA modulation, and kidney protection have yet to be established, warranting future investigations with advanced functional profiling and causal inference approaches. Finally, the safety profile of DHLCA, including potential off-target effects on FXR/TGR5-expressing tissues, remains to be defined. Further pharmacokinetic studies and long-term evaluations are needed to support its clinical translation.

## Conclusion

In summary, our findings demonstrate that DHLCA alleviates DKD by activating the TGR5/FXR signaling pathway and remodeling the GM. Beyond its renal and metabolic benefits, DHLCA exhibited no signs of hepatotoxicity and was associated with improved liver function. These results support its potential as a safe and effective therapeutic candidate for DKD, warranting further investigation in preclinical and clinical settings.

## Abbreviations

ADA, adenosine deaminase; ALB, albumin; ALP, alkaline phosphatase; ALT, alanine aminotransferase; AST, aspartate aminotransferase; AUC, area under the curve; BA, bile acid; BCA, bicinchoninic acid; BG, blood glucose; BSA, bovine serum albumin; BUN, blood urea nitrogen; CA, cholic acid; Ccr, creatinine clearance rate; CDCA-3Gln, chenodeoxycholic acid-3-*β*-D-glucuronide; CHE, cholinesterase; DBIL, direct bilirubin; DCA, deoxycholic acid; DKD, diabetic kidney disease; DM, diabetes mellitus; DHLCA, dehydrolithocholic acid; eGFR, estimated glomerular filtration rate; ESRD, end-stage renal disease; FBG, fasting blood glucose; FCP, fasting c-peptide; FDR, false discovery rate; FXR, farnesoid X receptor; GCA, glycocholic acid; GCDCA-3Gln, glycochenodeoxyche olic acid-3-O-*β*-glucuronide; GCDCA-3S, glycochenodeoxycholic acid-3-sulfate; GGT, gamma-glutamyl transferase; GLCA, glycolithocholic acid; GM, gut microbiota; GPCR, G-protein-coupled receptor; GO, gene ontology; GUDCA-3S, glycoursodeoxycholic acid-3-sulfate; Hb, haemoglobin; HbA1c, hemoglobin A1c; HC, healthy control; HDCA, hyodeoxycholic acid; HDL, high-density lipoprotein; FDR, false discovery rate; H&E, hematoxylin-eosin; HFD, high fat diet; IBIL, indirect bilirubin; IFTA, interstitial fibrosis and tubular atrophy; IQR, interquartile range; KIM-1, kidney injury molecule-1; LCA, lithocholic acid; LDA, linear discriminant analysis; LDH, lactate dehydrogenase; LDL, low-density lipoprotein; LEFSe, linear discriminant analysis effect size; LFD, low fat diet; MDCA, murideoxycholic acid; NCA, nor cholic acid; NGAL, neutrophil gelatinase-associated lipocalin; NLR, neutrophil to lymphocyte ratio; PAS, periodic acid-Schiff; RBC, red blood cell; RIPA, radioimmunoprecipitation assay; ROC, receiver operating characteristic curve analysis; RT-qPCR, real-time quantitative polymerase chain reaction; SCFA, short-chain fatty acid; Scr, serum creatinine; SD, standard deviation; STZ, streptozotocin; TBA, total bile acid; TBIL, total bilirubin; T2DM, type 2 diabetes mellitus; TC, total cholesterol; TG, triglycerides; TGR5, Takeda G protein-coupled receptor 5; TLCA, taurolithocholic acid; UACR, urine albumin-creatinine ratio; UPLC-MS/MS, ultrahigh-performance liquid chromatography tandem-mass spectrometry; WB, Western blot; WBC, white blood cell; 3DHCA, 3-dehydrocholic acid; 6-ketoLCA, 6-ketolithocholic acid.

## Data Sharing Statement

The datasets utilized and/or analyzed in this study can be obtained from the corresponding author upon reasonable request.

## Ethical Approval

This study was approved by the Third Affiliated Hospital of Ethics Committee of Soochow University (Ethics No: 2021–136, Approval date: 2021-03-10).

## Funding

This study was supported by grants from the National Natural Science Foundation of China (82000684), the Jiangsu Provincial Health Commission (M2024070), the Top Talent of Changzhou "The 14th Five-Year Plan" High-Level Health Talents Training Project (2022CZBJ003), Changzhou Sci & Tech Program (CJ20241111), and Changzhou Key Medical Discipline.

## Disclosure

All authors declare that there exists no potential competing interest. No benefits in any form have been received or will be received from a commercial party related directly or indirectly to the subject of this article. Hua Zhou, Xiaodie Mu and Huiyue Hu contributed equally to this work as Co-first authors. Jingting Jiang and Min Yang contributed equally to this work as Co-corresponding authors.

## References

1. Jager KJ, Kovesdy C, Langham R, et al. A single number for advocacy and communication-worldwide more than 850 million individuals have kidney diseases. *Kidney Int*. 2019;96(5):1048–1050. doi:10.1016/j.kint.2019.07.012
2. Zhang Q, Lu L, Wang J, et al. Metabolomic profiling reveals the step-wise alteration of bile acid metabolism in patients with diabetic kidney disease. *Nutr Diabetes*. 2024;14(1):85. doi:10.1038/s41387-024-00315-0
3. Li Z, Yuan H, Chu H, et al. The crosstalk between gut microbiota and bile acids promotes the development of non-alcoholic fatty liver disease. *Microorganisms*. 2023;11:2059. doi:10.3390/microorganisms11082059
4. Thibaut MM, Bindels LB. Crosstalk between bile acid-activated receptors and microbiome in entero-hepatic inflammation. *Trends Mol Med*. 2022;28(3):223–236. doi:10.1016/j.molmed.2021.12.006
5. Gai Z, Gui T, Hiller C, et al. Farnesoid X receptor protects against kidney injury in uninephrectomized obese mice. *J Biol Chem*. 2016;291(5):2397–2411. doi:10.1074/jbc.M115.694323
6. Wang XX, Edelstein MH, Gafter U, et al. G protein-coupled bile acid receptor TGR5 activation inhibits kidney disease in obesity and diabetes. *J Am Soc Nephrol*. 2016;27(5):1362–1378. doi:10.1681/ASN.2014121271
7. Chen B, Bai Y, Tong F, et al. Glycoursodeoxycholic acid regulates bile acids level and alters gut microbiota and glycolipid metabolism to attenuate diabetes. *Gut Microbes*. 2023;15(1):2192155. doi:10.1080/19490976.2023.2192155
8. Rowe JC, Summers SC, Quimby JM, et al. Fecal bile acid dysmetabolism and reduced ursodeoxycholic acid correlate with novel microbial signatures in feline chronic kidney disease. *Front Microbiol*. 2024;15:1458090. doi:10.3389/fmicb.2024.1458090
9. Collins SL, Stine JG, Bisanz JE, et al. Bile acids and the gut microbiota: metabolic interactions and impacts on disease. *Nat Rev Microbiol*. 2023;21(4):236–247. doi:10.1038/s41579-022-00805-x
10. Liu P, Jin M, Hu P, et al. Gut microbiota and bile acids: metabolic interactions and impacts on diabetic kidney disease. *Curr Res Microb Sci*. 2024;7:100315. doi:10.1016/j.crmicr.2024.100315
11. American Diabetes A. 2. classification and diagnosis of diabetes: standards of medical care in diabetes-2020. *Diabetes Care*. 2020;43:S14–S31. doi:10.2337/dc20-S002
12. Levey AS, Stevens LA, Schmid CH, et al. A new equation to estimate glomerular filtration rate. *Ann Intern Med*. 2009;150(9):604–612. doi:10.7326/0003-4819-150-9-200905050-00006
13. American Diabetes A. 11. microvascular complications and foot care: standards of medical care in diabetes-2021. *Diabetes Care*. 2021;44:S151–S167. doi:10.2337/dc21-S011
14. Farris AB, Adams CD, Brousaides N, et al. Morphometric and visual evaluation of fibrosis in renal biopsies. *J Am Soc Nephrol*. 2011;22(1):176–186. doi:10.1681/ASN.2009091005
15. Sakashita M, Tanaka T, Inagi R. Metabolic changes and oxidative stress in diabetic kidney disease. *Antioxidants*. 2021;10(7):1143. doi:10.3390/antiox10071143
16. Yuan Y, Huang L, Yu L, et al. Clinical metabolomics characteristics of diabetic kidney disease: a meta-analysis of 1875 cases with diabetic kidney disease and 4503 controls. *Diabetes Metab Res Rev*. 2024;40(3):e3789. doi:10.1002/dmrr.3789
17. Wang XX, Wang D, Luo Y, et al. FXR/TGR5 dual agonist prevents progression of nephropathy in diabetes and obesity. *J Am Soc Nephrol*. 2018;29(1):118–137. doi:10.1681/ASN.2017020222
18. Watanabe M, Houten SM, Mataki C, et al. Bile acids induce energy expenditure by promoting intracellular thyroid hormone activation. *Nature*. 2006;439(7075):484–489. doi:10.1038/nature04330
19. Kaya D, Kaji K, Tsuji Y, et al. TGR5 activation modulates an inhibitory effect on liver fibrosis development mediated by anagliptin in diabetic rats. *Cells*. 2019;8(10):1153. doi:10.3390/cells8101153
20. Yang Z, Xiong F, Wang Y, et al. TGR5 activation suppressed S1P/S1P2 signaling and resisted high glucose-induced fibrosis in glomerular mesangial cells. *Pharmacol Res*. 2016;111:226–236. doi:10.1016/j.phrs.2016.05.035
21. Chen C, Zhang B, Tu J, et al. Discovery of 4-aminophenylacetamide derivatives as intestine-specific farnesoid X receptor antagonists for the potential treatment of nonalcoholic steatohepatitis. *Eur J Med Chem*. 2024;264:115992. doi:10.1016/j.ejmech.2023.115992
22. Dehondt H, Marino A, Butruille L, et al. Adipocyte-specific FXR-deficiency protects adipose tissue from oxidative stress and insulin resistance and improves glucose homeostasis. *Mol Metab*. 2023;69:101686. doi:10.1016/j.molmet.2024.101961
23. Hasan IH, Shaheen SY, Alhusaini AM, et al. Simvastatin mitigates diabetic nephropathy by upregulating farnesoid X receptor and Nrf2/HO-1 signaling and attenuating oxidative stress and inflammation in rats. *Life Sci*. 2024;340:122445. doi:10.1016/j.lfs.2024.122445

24. Balint L, Socaciu C, Socaciu AI, et al. Metabolites potentially derived from gut microbiota associated with podocyte, proximal tubule, and renal and cerebrovascular endothelial damage in early diabetic kidney disease in T2DM patients. *Metabolites*. 2023;13(8):893. doi:10.3390/metabo13080893
25. Balint L, Socaciu C, Socaciu AI, et al. Quantitative, targeted analysis of gut microbiota derived metabolites provides novel biomarkers of early diabetic kidney disease in type 2 diabetes mellitus patients. *Biomolecules*. 2023;13(7):1086. doi:10.3390/biom13071086
26. Zuo K, Fang C, Gao Y, et al. Suppression of the gut microbiota–bile acid– FGF19 axis in patients with atrial fibrillation. *Cell Prolif*. 2023;56(11):e13488. doi:10.1111/cpr.13488
27. Choi H, Bae SJ, Choi G, et al. Ninjurin1 deficiency aggravates colitis development by promoting M1 macrophage polarization and inducing microbial imbalance. *FASEB J*. 2020;34(6):8702–8720. doi:10.1096/fj.201902753R
28. Luo Z, Xu J, Gao Q, et al. Study on the effect of licochalcone A on intestinal flora in type 2 diabetes mellitus mice based on 16S rRNA technology. *Food Funct*. 2023;14(19):8903–8921. doi:10.1039/d3fo00861d
29. Dong W, Zhao Y, Li X, et al. Corn silk polysaccharides attenuate diabetic nephropathy through restoration of the gut microbial ecosystem and metabolic homeostasis. *Front Endocrinol*. 2023;14:1232132. doi:10.3389/fendo.2023.1232132
30. Yang JY, Lee YS, Kim Y, et al. Gut commensal Bacteroides acidifaciens prevents obesity and improves insulin sensitivity in mice. *Mucosal Immunol*. 2017;10(1):104–116. doi:10.1038/mi.2016.42
31. Shen Q, Zhong YT, Liu XX, et al. Platycodin D ameliorates hyperglycaemia and liver metabolic disturbance in HFD/STZ-induced type 2 diabetic mice. *Food Funct*. 2023;14(1):74–86. doi:10.1039/d2fo03308a
32. Cheng W, Zhou X, Jin C, et al. Acid-base transformative HADLA micelles alleviate colitis by restoring adaptive immunity and gut microbiome. *J Control Release*. 2023;364:283–296. doi:10.1016/j.jconrel.2023.10.039
33. Nakamoto N, Sasaki N, Aoki R, et al. Gut pathobionts underlie intestinal barrier dysfunction and liver T helper 17 cell immune response in primary sclerosing cholangitis. *Nat Microbiol*. 2019;4(3):492–503. doi:10.1038/s41564-018-0333-1
34. Van Nierop FS, Scheltema MJ, Eggink HM, et al. Clinical relevance of the bile acid receptor TGR5 in metabolism. *Lancet Diabetes Endocrinol*. 2017;5(3):224–233. doi:10.1016/S2213-8587(16)30155-3
35. Lefebvre P, Cariou B, Lien F, et al. Role of bile acids and bile acid receptors in metabolic regulation. *Physiol Rev*. 2009;89(1):147–191. doi:10.1152/physrev.00010.2008